Feasibility of a New Ironless-stator Axial Flux Permanent Magnet Machine for Aircraft Electric Propulsion Application

Zhuoran Zhang, senior member, *IEEE*, Weiwei Geng, member, *IEEE*, Ye Liu, student member, *IEEE*, and Chen Wang, student member, *IEEE*

(Invited)

***Abstract*— With the development of aviation electrification, higher demands for electrical machines are put forward in aircraft electric propulsion systems. The aircraft electric propulsion requirements and propulsion motor features are analyzed in this paper. Comparing with conventional PM machines, ironless stator axial flux permanent magnet (AFPM) machine topologies with Litz wire windings allow designs with higher compactness, lightness and efficiency, which are suitable for high-frequency and high-power density applications. Based on the motor requirements and constraints of aircraft electric propulsion systems, this paper investigates a high-power 1 MW multi-stack ironless stator AFPM machine, which is composed of four 250kW modular motors by stacking in axial. The design guidelines and special attentions are presented, in term of electromagnetic, thermal, and mechanical performance for the high-frequency coils and Halbach-array PM rotor. Finally, an ironless stator AFPM motor is manufactured, tested and evaluated with the consideration of cost and processing cycle. The results show that the output power is up to 53.8kW with 95% efficiency at 9000r/min at this stage. The proposed ironless stator AFPM machine with oil immersed forced cooling proves to be a favorable candidate for application in electric aircraft as propulsion motors.**

***Index Terms*—Axial flux machine, electric aircraft, electric propulsion, ironless stator permanent magnet machine, oil cooling.**

I. INTRODUCTION

THE concept of aircraft electric propulsion gradually becomes the main melody of aviation industry development. With the fast development of air traffic, the environmental impact of air traffic has caught more and more attention, and aircraft electrical power systems have developed substantially [1]-[3]. NASA has proposed strict goals for fuel consumption, NOx emission and noise for the next three generations of aircraft in shaping its technology roadmaps, namely N+1, N+2 and N+3 [1]. Table I gives these detailed goals.

TABLE I
NASA SUBSONIC AIRLINE PERFORMANCE GOALS

	N+1 (~2015)	N+2 (~2020)	N+3 (~2030)
Noise	-32dB	-42dB	-71dB
NOx emission	-60%	-75%	<-80%
Fuel consumption	-33%	-50%	<-70%

The development of aero engine technology is one of the main approaches to realize the subsonic airline performance goals. However, it is difficult to realize the goals of N+3 due to the low energy conversion efficiency of propulsion system and secondary power system. In this context, the ideas of more electric aircraft (MEA) and electric propulsion technology emerge.

In order to improve the reliability and maintenance of the secondary power, the capacity of electrical power is raised to replace the hydraulic, pneumatic and mechanical power, defined as MEA. The power system is simplified in MEA, which brings some distinct advantages, including reduction of aircraft weight, low operating costs, efficient energy management, high reliability and maintenance, and low environmental impact [4].

Developing the electric propulsion system, especially the distributed electric propulsion system, is considered as a feasible method to realize N+3. Many relevant research studies have been conducted. Furthermore, a number of aircraft electric propulsion systems require high-speed and high-power ratings with the constraints, including space, weight and efficiency [5]-[9]. High power density electrical machines are always included as key underlying components in electric propulsion systems.

Considering the higher demand for efficiency and torque density of electric machines in aircraft electric propulsion systems, permanent-magnet (PM) machines are the go-to solutions, including radial-flux PM machines and axial-flux PM (AFPM) machines. AFPM machine has attracted more and more research efforts in the past decades due to the high torque density, high efficiency and high compactness. AFPM machines are more suitable for drive applications for favorable electromagnetic characteristics, such as high torque and power density.

Ironless stator AFPM machines are considered as a prominent branch of AFPM machines, which have attracted

Manuscript was submitted for review on 01, February, 2019.

This work was supported in part by National Natural Science Foundation for Excellent Young Scholar of China under Award 51622704, in part by Jiangsu provincial key research and development project under Award BE2017160.

The authors are with the Center for More-Electric-Aircraft Power Systems, Nanjing University of Aeronautics and Astronautics, Nanjing, China. (e-mail: apsc-zzr@nuaa.edu.cn; gww0424@163.com; liuye_nuaa@163.com; wangchen1071@163.com).

Digital Object Identifier 10.30941/CESTEMS.2019.00005

much academic and industrial attention due to the high efficiency and favorable torque-current characteristic. Thus, ironless stator AFPM machines are deemed as good candidates in some applications, including vehicle propulsion system, aerospace, and high-speed FESS [10]-[13]. However, due to low air-gap flux density, the low torque density is always the bottleneck of pervasive application. Compared with various machine geometries, the axial flux topology with dual rotors and internal stator presents higher torque density. Furthermore, PM rotors with magnetic flux-concentrating effect, such as Halbach-array structure, can improve air-gap flux density effectively. What's more, the cooling system and structure design of the ironless stator ensure the sufficient heat dissipation under high electrical loads and the mechanical strength at high speed.

This paper presents a brief review of electric power systems of distributed electric propulsion aircraft, with a focus on the discussion of candidate motors. The applicability of ironless stator AFPM machines to a distributed electric propulsion system for aircraft applications is proposed and introduced briefly. A multi-disk solution of 1 MW ironless stator AFPM machine is proposed and a modular sub-motor with 250kW output power is designed. The finite element analysis (FEA) simulation results are given and discussed, which present high power density characteristic. Finally, a reliable topology of ironless stator AFPM motor prototype is successfully developed and measured to meet the desired consequence of strength and cooling. It indicates that the proposed construction of ironless stator is reliable, which provides a productive implement approach of ironless stator AFPM machines for electric propulsion aircraft application.

II. Aircraft Electric Propulsion Requirements and Propulsion Motor Approach

A. Aircraft Electric Propulsion Requirements

The concept of electric drive or propulsion system has been widely used in hybrid and electric vehicles, and many mature commercial products of electric drive or propulsion are emerging in the automotive industry. There are numerous electric drive or propulsion system architectures which have been proposed for electric propulsion powertrains. In this paper, from the perspective of power output composition, three hybrid power systems combining batteries and gas turbine engines for propulsion are shown in Fig. 1.

1) Fig.1(a) gives a typical power architecture of electric propulsion system: mechanical parallel by gear box for hybrid power. In this architecture, the engine and the motor jointly drive the bypass fans or propellers through the transmission device. The propulsion motor is used to accommodate with the engine to operating at the state of the best fuel economy. As shown in Fig.1(a), with the transmission device as the medium, the propulsion motor can work in generating and motoring modes. In fact, the propulsion motor just acts as an energy balance regulator, However, because the engine is directly coupled to the aircraft propeller drive shaft through the transmission device, hence, this power architecture is defined as a weak mixing of hybrid power. However, the main drive of the engine and existence of the transmission device limit the further improvement of efficiency and the flexibility of power system layout.

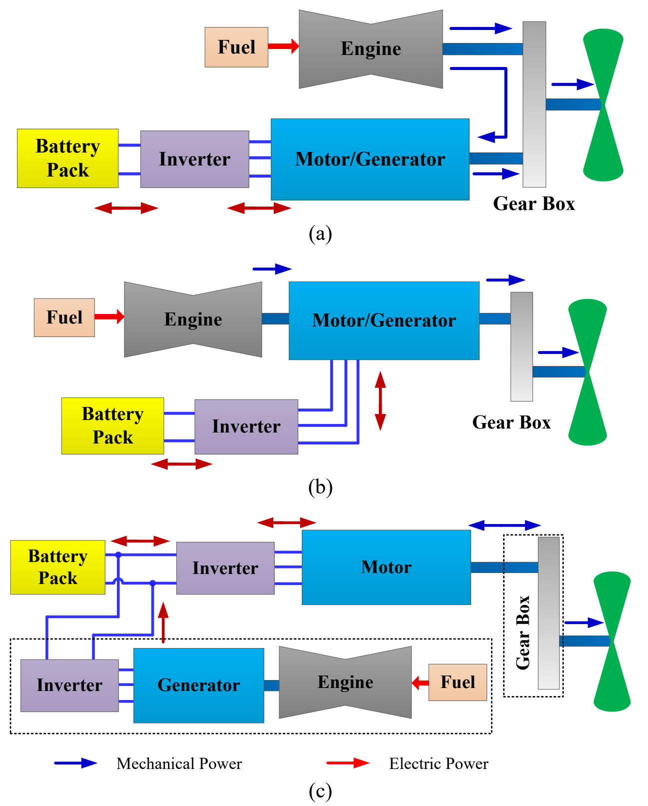

Fig. 1. Classification of power electric propulsion system architectures for propeller or bypass fan of aircraft. (a) Mechanical parallel by gear box for hybrid power. (b) Mechanical series with transmission shaft. (c) Electrical parallel between generator systems and battery.

2) Fig.1(b) shows the mechanical series power architecture with transmission shaft. The engine and propulsion motor are coaxially mounted and mechanically coupled through the drive shaft. The power proportion of the propulsion motor and engine directly determines the degree of hybridization of oil fuel and battery power.

3) Fig.1(c) gives a more acceptable power architecture, which is defined as electrical parallel between generator systems and battery. The power input of bypass fans or propellers is only from the propulsion motor. It can eliminate the gear mechanism by means of direct drive and reduce the weight of the motor system by using a high-speed motor with a reducer. The propulsion motor can be powered mainly by the battery or turboelectric generator system. If the turboelectric generator system (as shown in dashed box) is canceled, it will turn into an all-electric propulsion system.

It is noted that electrical machines occupy a pivotal position whether in the hybrid or electric propulsion systems. The electric propulsion system needs a motor to provide the equivalent thrust of the original engine. Table II gives the thrust of several typical aircraft types. As shown in Fig. 2 [14], the

TABLE II
THRUST OF DIFFERENT AIRCRAFT TYPES

Types	Maximum passenger capacity	Engine	Thrust
Airbus A380	555	Trent 900 or GP 7200*4	311*4 kN
Boeing 787	330	Trent 1000*2	340*2 kN
Airbus A320	186	CFM56-5*2	120*2 kN
Bombardiern CRJ-900	90	CF34*2	65*2 kN

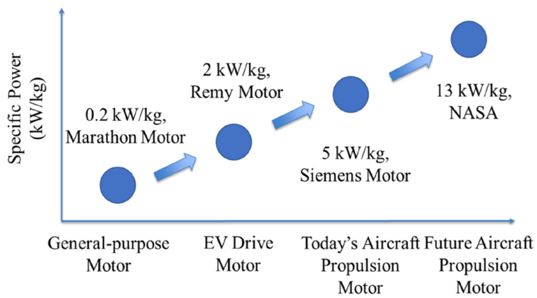

Fig. 2. Future requirements of electric machine for electric propulsion aircraft application [14].

design speeds and power ratings of the machines for electric propulsion aircraft application reach an almost critical state, which brings a great challenge to motor design.

B. Propulsion Motors

Based on the survey results, the high-power machines are listed in Table III. Although the surveyed high-power machines do not meet all the requirements of aircraft electric propulsion systems, their design methods and data can help us accelerate the design procedure of high-power machines for electric propulsion systems. It can be seen that high-speed and high-power machines mainly includes: radial flux permanent-magnet (RFPM) machines, induction machines (IMs), switched reluctance machines (SRMs), and AFPM machines. The power density is closely related to the cooling system and operating speed. Compared with the other topologies, the RFPM machines have higher power density.

III. IRONLESS STATOR AFPM MOTORS FOR AIRCRAFT ELECTRIC PROPULSION

A. Design considerations of propulsion motor

The aircraft electric propulsion systems require large rated power with constraints, including space, weight, and efficiency. The achievement of 13 kW/kg power density is regarded as a key milestone for megawatt-class propulsion motors in the development of future hybrid-electric aircraft [15]. To achieve high-power ratings with a reduced weight, propulsion motors are always designed with high operating speed. Parasitic effects, including mechanical strength, vibration and noise, always become a significant concern when designing a high-speed electrical machine. In order to satisfy the high requirements of aircraft electric propulsion systems, the main design considerations of propulsion motor are analyzed and described as follows.

TABLE III
HIGH POWER AND HIGH SPEED MACHINE

Topology	Speed /rpm	Power /kW	Power density /kW/kg	Cooling system	Ref.no.
RFPM	15000	5000	--	Indirect water	[16]
RFPM	6000	3750	3.2[b]	direct water	[17]
RFPM	20000	1500	8.4[a]	Indirect water	[18]
RFPM	15000	8000	8.9[a]	Forced air	[19]
RFPM	15000	1000	13.5[a]	Forced air	[2]
IM	15000	2000	2.0[b]	Indirect water and forced air	[20]
IM	12000	8000	1.6[b]	Forced air	[21]
IM	60000	300	2.3[b]	Indirect water and forced air	[22]
IM	10000	6750	1.8[b]	--	[23]
IM	20000	15000	2.2[b]	Indirect water and forced air	[24]
SRM	22000	250	4.5[b]	Direct oil, hollow shaft	[25]
SRM	18000	250	3.3[b]	--	[26]
AFPM	4000	100	4.9[a]	Indirect water	[27]
AFPM	5000	150	1.9[b]	Indirect liquid	[28]
AFPM	1846	110	1.1[b]	Air	[29]

[a] Estimated SP from the mass of only active materials
[b] Estimated SP from the machine geometrical dimensions

(1) High power density topologies

High power density motor topology is the key technology to propulsion motors. The high-speed rotor often needs a high tensile sleeve, which causes an increase of main air-gap length in conventional inner-rotor PM machines. The increase of main air-gap length would lead to a decrease in electromagnetic performance due to the decrease of air-gap flux density. It is known that both outer-rotor and AFPM machines are featured of high torque and power density. Meanwhile, the sleeve would not affect the air gap and the mechanical design is relatively easy in outer-rotor and AFPM machines. Halbach array can be used to reduce the weight of rotor yoke and improve the air-gap flux density further.

(2) Loss analysis and cooling system design

One of the key challenges of high power density propulsion motor is the optimization of loss and efficiency. In conventional PM machines, the losses mainly include stator core loss, armature winding copper loss, PM loss, sleeve loss, rotor core loss and stray loss. The slotless stator structure can be used to reduce stator core loss, rotor core loss and PM loss. The Halbach array can also reduce the harmonic components of air-gap flux density, which can reduce the losses further. The large losses in a compact space would cause a serious temperature rise, which needs a high-performance cooling system design.

(3) Modularity and fault-tolerance

It is known that the design, manufacture and experiments of high-power motor are difficult and expensive. Fault tolerance is always a key issue in PM machine design, especially in some safety-critical applications. The large-power motor can be modularized by breaking the whole up into several modular motors, which can be controlled by several independent control units to realize fault-tolerance.

B. High-power propulsion motor design

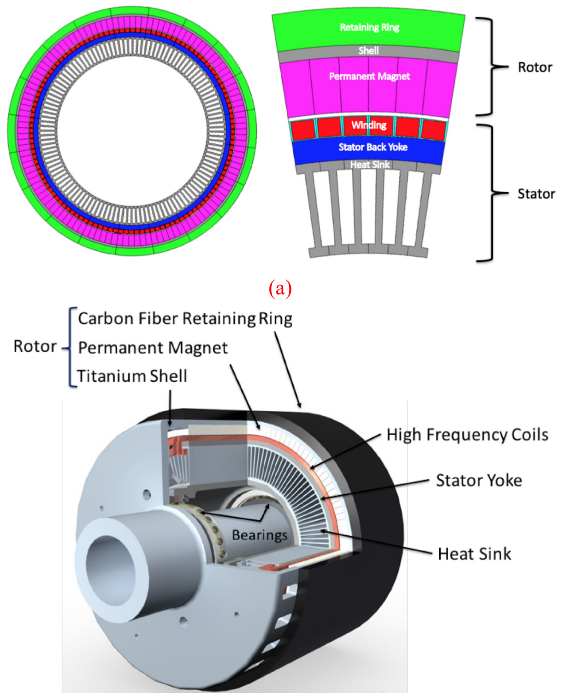

Fig. 3. The outer-rotor permanent magnet motor in [30]. (a) Axial view. (b) 3D description.

TABLE IV [33]
THE OUTER-ROTOR SLOTLESS PERMANENT MAGNET PROPULSION MOTOR SPECIFICATIONS

Parameter	Value
Rated power	1.0 MW
Rated speed	15000 r/min
Poles/slots	20/120
No. of phase	3
No. of turns	3
No. of parallel circuits	10
Air gap	1.15 mm
Machine outer radius	159.13 mm
Stack length	241.4 mm
core material	silicon steel
PM remanent B	1.2 T
shell material	titanium
—	aermet

Considering these constraints and design considerations of aircraft electric propulsion systems, high-power propulsion motor design is challenging. In [30]-[33], Kiruba Haran *et al.* designed a 1MW, 15000r/min outer-rotor slotless PM propulsion motor, as shown in Fig. 3. Table IV presents the specifications of the outer-rotor slotless PM propulsion motor.

With respect to the space constraint and fault-tolerance, a 1MW, 15000r/min ironless stator AFPM propulsion motor is proposed and designed with the same space constraint of the outer-rotor PM motor. As shown in Fig. 4, the 1MW, 15000r/min AFPM motor consists of four 250kW, 15000r/min modular AFPM motors. The physical separation between the four modular AFPM motors realizes favorable fault-tolerance. In order to simplify the design, manufacture and experiment procedures, the validation of the 1MW, 15000r/min ironless stator AFPM propulsion motor can be demonstrated by a 250kW, 15000r/min modular AFPM motor.

The specifications of the proposed ironless stator AFPM

TABLE V
PROPOSED IRONLESS STATOR AFPM MOTOR SPECIFICATIONS

Parameter	Value
Rated power	1.0 MW (250kW*4)
Rated speed	15000 r/min
Poles/slots	10/12
No. of phase	3
No. of coil-group	5
Air gap	1 mm
Machine outer radius	160 mm
Effective axial length	240 mm (60mm*4)
PM remanent B	1.2 T

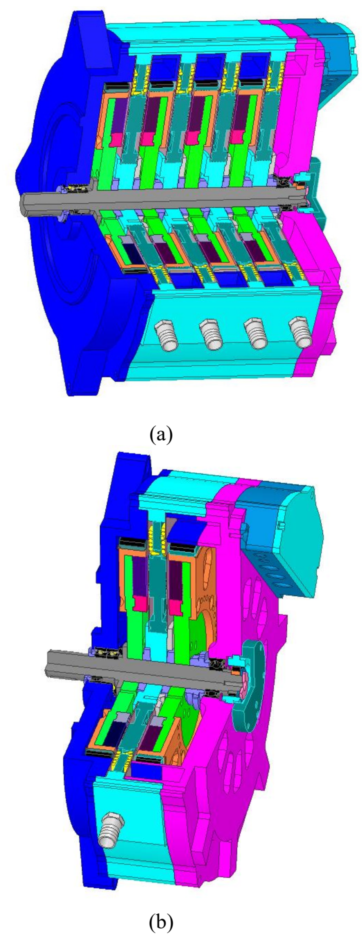

Fig. 4. Proposed axial flux permanent magnet motor topology. (a) Integrated structure. (b) Module structure.

TABLE VI
PRIMARY PARAMETERS OF 250KW MODULAR AFPM MOTOR

Parameter	Value
Number of Slot/pole	12/10
Outer Radius	320 mm
Inner Radius	200 mm
Non-magnetic distance	20 mm
Axial thickness of PM	25 mm
Actual air-gap	1.0 mm
Axial length of one coil	6 mm
Radians of one coil	0.049
Number of coil-group	5
Midline pitch radian of coil-group	0.157
Layer Number of stator windings.	2
Output Power	250 kW
Rated speed	15000 rpm
Phase back-EMF	200 V
Current density	<25 A/mm^2
Effective Axial-Length	60 mm

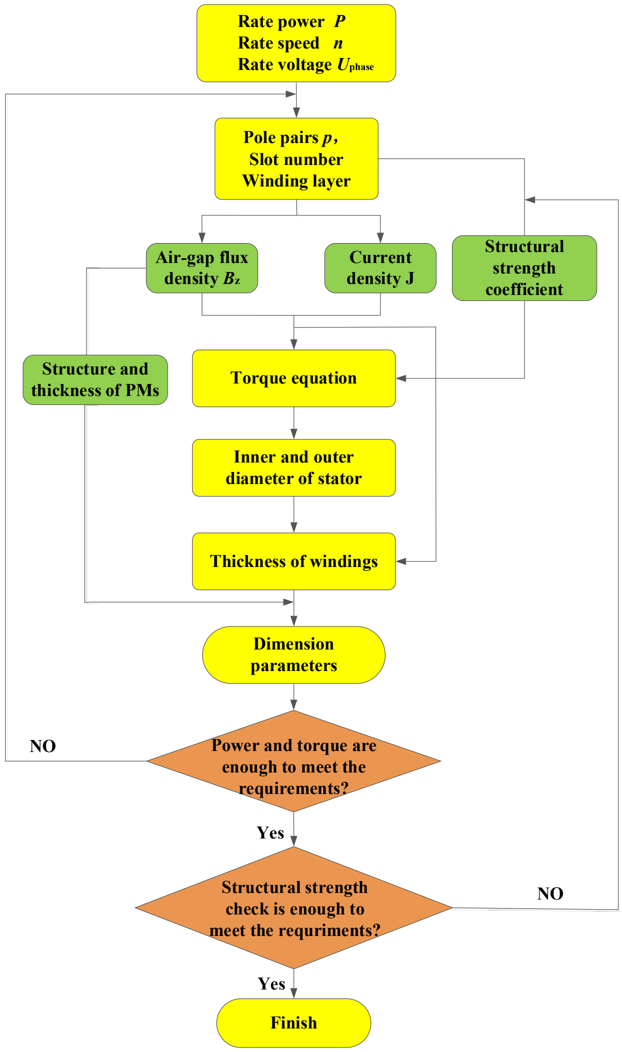

Fig. 5. Flowchart of the proposed machine design.

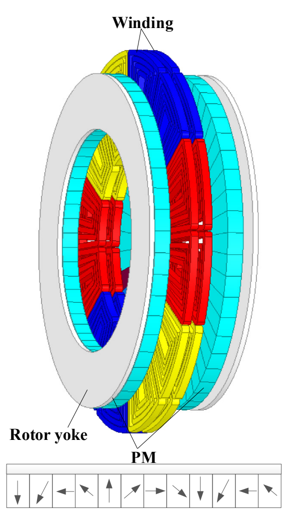

Fig. 6. Three-dimensional model of the proposed 250kW machine.

propulsion motor solution are shown in Table V. The volume of the proposed ironless stator AFPM propulsion motor is consistent with that of the outer-rotor slotless PM propulsion motor. The axial length can be optimized further by integrated

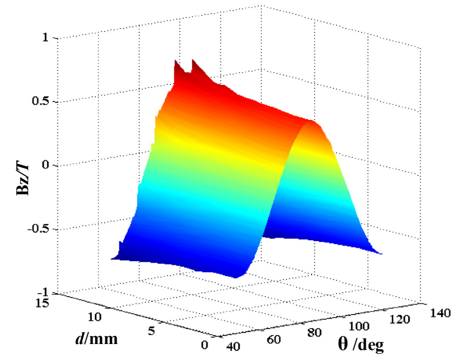

Fig. 7. The air-gap flux density.

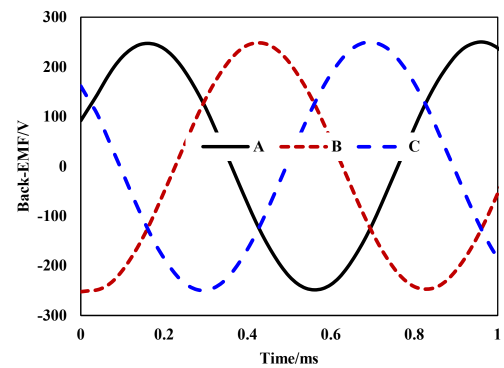

Fig. 8. Back-EMF waveforms of the ironless stator AFPM machine.

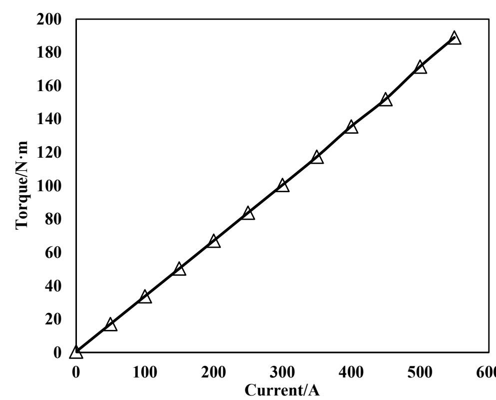

Fig. 9. Torque versus different phase current.

design.

IV. Development of 250 kW Ironless Stator AFPM Modular Motor

A. Electromagnetic design

If the distribution of the air-gap magnetic field is sinusoidal, the average flux density for AFPM machines can be calculated by

$$\begin{aligned} B_{avg} &= \frac{1}{\pi/p-0}\int_0^{\pi/p} B_{g1}\sin(p\alpha)d\alpha \\ &= -\frac{p}{\pi}B_{g1}\left[\frac{1}{p}\cos(p\alpha)\right]_0^{\pi/p} \\ &= -\frac{1}{\pi}B_{g1}[\cos\pi-\cos 0] = \frac{2}{\pi}B_{g1} \end{aligned} \tag{1}$$

where p is pole pairs, B_{g1} is the fundamental component

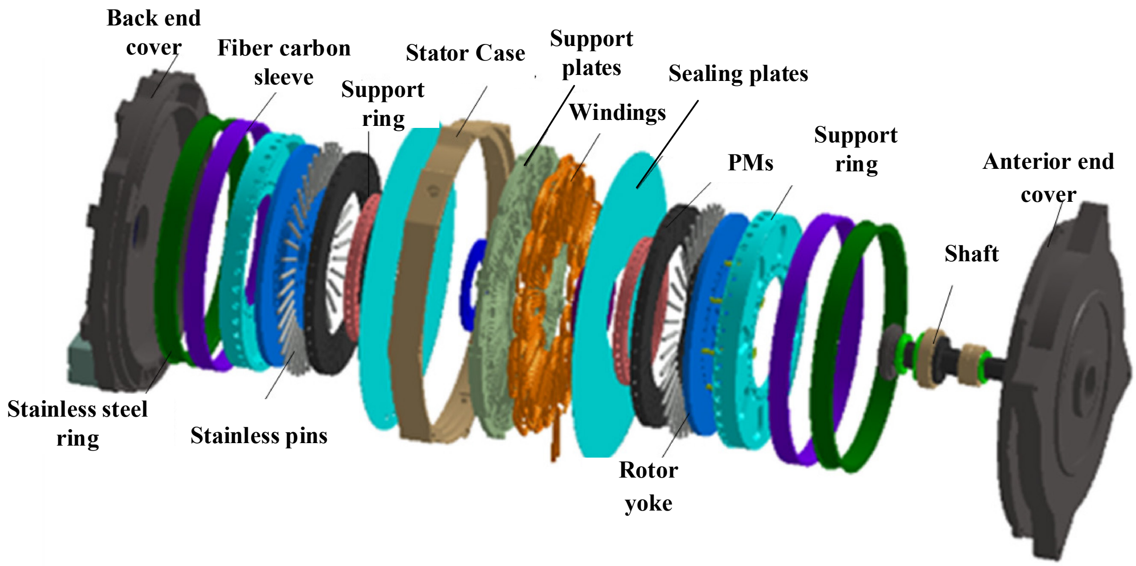

Fig. 10. The general structure of ironless stator AFPM machine.

amplitude of air-gap flux density.

The phase back electromotive force (EMF) can be predicted by the following equation.

$$E_{ph} = 2\pi f N_{ph} k_w \phi_f = 2\pi f N_{ph} k_w \frac{B_{g1}(r_o^2 - r_i^2)}{p_n} = \frac{1}{30}\pi n N_{ph} k_w B_{g1}(r_o^2 - r_i^2) \quad (2)$$

where N_{ph} is number of turns per phase winding per layer, n is rotational speed, k_w is winding factor.

For the AFPM machines, the Lorentz magnetic force on single conductor in axial magnetic field can be expressed as

$$\vec{F} = (R_o - R_i)\cdot(\vec{i}\times\vec{B}) \quad (3)$$

The Lorentz magnetic force on total windings in the radial direction can be calculated by the following equation.

$$F_1(r) = 2p\int_0^{\pi/p} \hat{B}_{g1}\cos(p\theta-\alpha)\frac{3}{2}I\sqrt{2}\frac{N_s}{2}\sin(p\theta)d\theta dr \quad (4)$$

The electromagnetic torque can be calculated by

$$T_1 = \frac{3}{8}\sqrt{2}\pi\hat{B}_{g1} I N_s (r_o^2 - r_i^2)\sin(\beta) \quad (5)$$

The power equation is derived as

$$P = T_1\cdot\Omega = \frac{3}{8}\sqrt{2}\hat{B}_{g1} I N_S (r_o^2 - r_i^2)\cdot\sin\beta\cdot\frac{2\pi n}{60} = \frac{\sqrt{2}}{80}\pi^2 k_w \hat{B}_{g1} J \frac{1}{k_{ma}k_{mc}} l_s r_i (r_o^2 - r_i^2)\cdot n \quad (6)$$

where J is current density, l_s is axial length, k_{ma} is axial strength coefficient, k_{mc} is peripheral strength coefficient.

On the basis of sizing equation, the basic calculation process is shown in Fig. 5. According to the size of outer-rotor PM machine in Table IV, the calculated results of ironless stator AFPM machine are given in Table VI. Fig. 6 shows the FEA model of 250kW modular AFPM motor with internal ironless stator. In order to improve the air-gap flux density, the Halbach-array is adopted in the design and composed of forty PM pieces. The magnetization direction of the forty PM pieces varies 45° in turn.

Fig. 7 shows the three-dimensional air-gap flux density distribution with respect from the center line of the air gap. It can be seen that the air-gap flux density waveform is relatively sinusoidal.

Fig. 8 gives the phase back EMF waveform of ironless stator AFPM machine at 15000r/min, it can be seen that the fundamental amplitude of back-EMF for the ironless stator AFPM machine is about 390V.

The average torque variation of the ironless stator AFPM machine along with phase current is shown in Fig. 9. The torque increases linearly with phase current in the ironless stator AFPM machine. The torque-current ratio is about 0.34N·m/A and the output power is about 250kW when the phase current is about 450A at 15000r/min.

B. Mechanical Design Considerations and High-speed Operational Issues

The mechanical construction of the proposed ironless stator AFPM machine is shown in Fig. 10. When the speed is increased further in pursuit of high power density design, the mechanical design constraints would become more serious and even limit the design.

In order to improve the mechanical strength of rotor, a new hybrid protective sleeve is proposed. The carbon fiber sleeve is mounted on the stainless steel sleeve to enhance mechanical strength further. Since the carbon fiber material is sensitive to bending force, the carbon fiber sleeve avoids direct contact with the stainless steel screws in rotor design.

The tangential stress of PM and the equivalent stress of dual rotors at 90℃, 15000r/min are analyzed by 3D FEM, and the results are shown in Fig. 11. It can be seen that the maximum tangential stress of PM is about 48.9MPa, and the maximum equivalent stress of dual rotors is about 355MPa. The maximum allowed compressive stress of rotor is about 650MPa, and the maximum allowed tensile stress of PM is 80MPa.

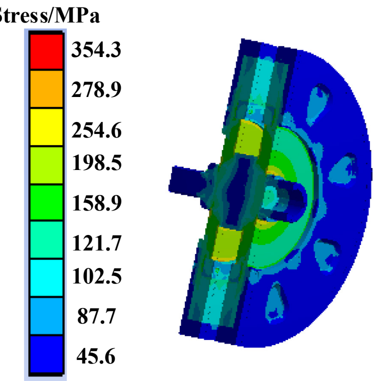

(a)

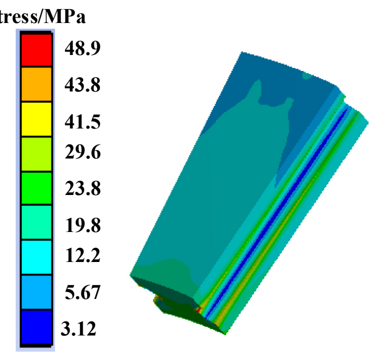

(b)

Fig. 11. The stress of ironless stator AFPM machine rotor. (a) Dual-rotor. (b) PM.

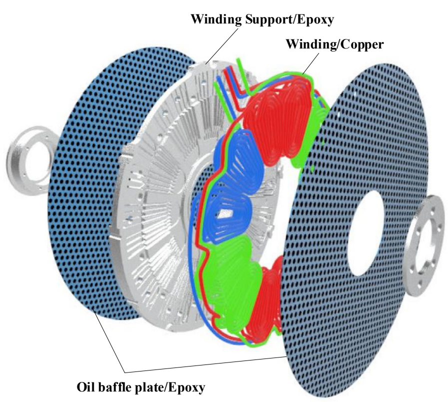

Fig. 12. Construction of ironless stator.

C. Oil immersed Forced cooling

In order to enhance the output performance of machine, an oil immersed forced cooling system is applied in the machine. The aim of oil immersed force cooling system is to transfer the heat of the copper losses and eddy losses to the oil.

The construction of the ironless stator and winding shape is shown in Fig. 12. In order to improve electromagnetic performance, each phase winding divided into two layers is fixed with epoxy support. All windings are placed in the cooling oil, the cooling oil is sealed with two epoxy baffle plates.

The inlet velocity is 1.2m/s, and the inlet flow rate is 15L/min. The velocity distribution of cooling oil in each part of stator is shown in Fig. 13. It can be seen that the cooling oil flows along the windings and winding framework after the cooling oil is entered into the stator. The overall velocity is about 0.5~1.0m/s because of the winding arrangement is dense. The velocity of inlet and outlet exceeded 1.5m/s since the turbulence exists.

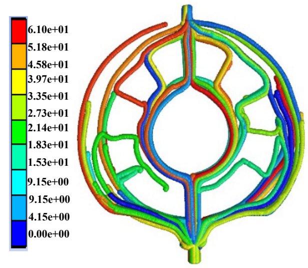

(a)

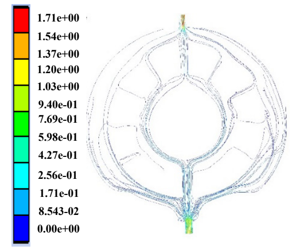

(b)

Fig. 13. Stator cooling oil fluid field. (a) Cooling oil flow line. (b) Cooling oil flow.

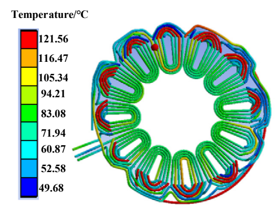

(a)

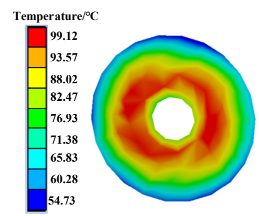

(b)

Fig. 14. Temperature distribution of stator under 15000 r/min, 250kW. (a) Winding. (b) Oil baffle plate.

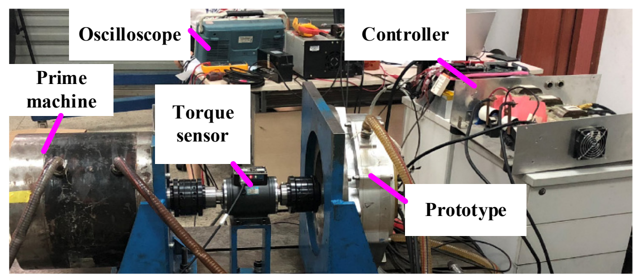

Fig. 15. Prototype of the ironless stator AFPM machine and test platform.

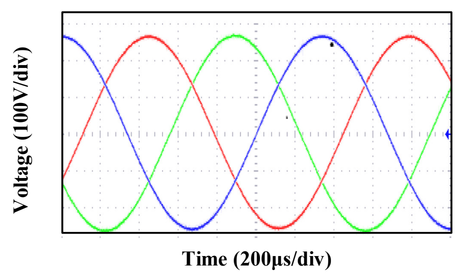

(a)

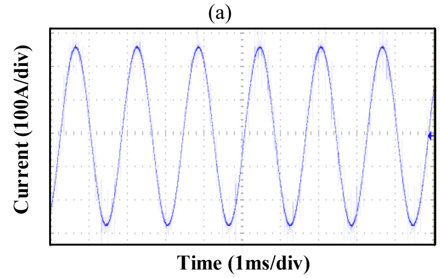

(b)

Fig. 16. Experimental results under generating operation. (a) Waveforms of back-EMF with no-load at 9000r/min. (b) Loading waveform of the phase current at 9000r/min.

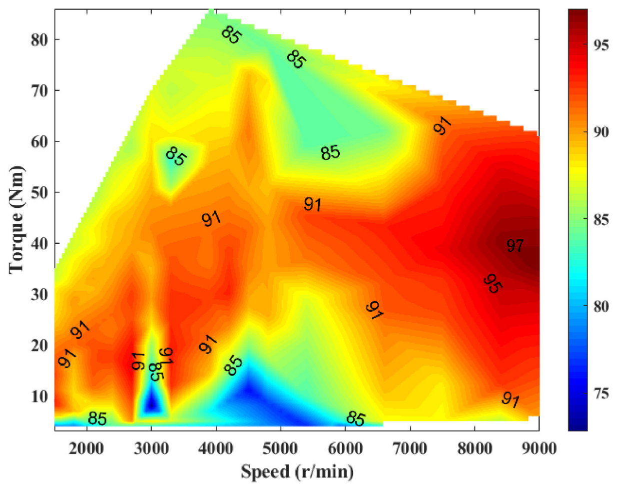

Fig. 17. Measured efficiency map of the prototype machine.

The temperature distribution of the windings and oil baffle plate is shown Fig. 14. It can be seen that the temperature of winding end is about 100℃, and the temperature of winding is about 65℃ when the oil flow in the slot is much larger than the end of winding. In particular, the eddy loss exists in the active part of the winding, because the loss at the end of windings is less than the loss at the active part of the windings. So the simulation results of temperature distribution can only serve as a reference.

D. Experimental verification

To validate the feasibility of the ironless stator AFPM machine design and analysis method, the prototype of a 50kW, 9000r/min ironless stator AFPM machine with Halbach-array PM rotor is manufactured with the consideration of cost and processing cycle. The prototype and test platform are shown in Fig. 15. The prototype is driven by a 12000r/min, 100kW PMSM.

The prototype machine has been tested up to 9000r/min and the three-phase back-EMFs are measured at no load. The machine runs at the speed of 9000r/min for two hours, and the three-phase back-EMF is shown in Fig. 16(a). It can be seen that the fundamental amplitude of back-EMF is about 261V.

In addition, the electromagnetic characteristics at the rated load are tested. Fig. 16(b) shows the measured phase current waveform at 9000r/min. Fig. 17 shows the measured efficiency and output power under different load currents at 9000r/min. It is noted that the value of output power increases linearly with the increase of load current, and the maximum output power is about 53.8kW. It is worth noting that the efficiency is increased significantly at first and then reduced when the load current is increased. The maximum efficiency of the prototype ironless stator AFPM machine is about 97.4% when the load current is about 120A.

V. Conclusion

This paper has presented a feasible technology solution of propulsion motor for aircraft electric propulsion applications. A new ironless stator AFPM machine with oil immersed forced cooling system is proposed as a favorable candidate because of the advantages of high efficiency and power density, as well as the axial modularity and fault-tolerance.

The concept and design of a high-power 1 MW multi-stack ironless stator AFPM machine have been presented, which is composed of four 250kW modular motors by stacking in axial. The detailed electromagnetic, structural considerations and thermal design are presented and discussed. The research results indicate that the power density and efficiency of the proposed multi-stack ironless stator AFPM machine are over 13kW/kg and 96%, respectively. Furthermore, the unit prototype machine has been developed and tested up to 53.8kW at 9000 r/min. The maximum efficiency reaches 97.4% when the current density is about 10A/mm². Because the oil immersed forced cooling system is adopted, the electric load of ironless stator can be further increased by three times to improve torque density, which lays a good foundation for MW-level propulsion motor design and implementation.

References

[1] Davies K, Norman P, Jones C, et al, “A review of turboelectric distributed propulsion technologies for N+3 aircraft electrical systems” in *Power Engineering Conf.*, Dublin, 2013, pp. 1-5.

[2] Morioka, Noriko, Michiya Takeuchi, and Hitoshi Oyori, “Moving to an All-Electric aircraft system,” *IHI Engineering Review*, vol. 47, no. 1, pp. 33-39, Sep., 2014.

[3] Felder J L, Brown G V, Kim H D, et al. Turboelectric distributed propulsion in a hybrid wing body aircraft: ISABE-2011-1340 [R]. Cleveland, Ohio: NASA Glenn Research Center, 2011.

[4] Z. Zhang, Y. Liu and J. Li, "A HESM-Based Variable Frequency AC Starter-Generator System for Aircraft Applications," in *IEEE Transactions on Energy Conversion*, vol. 33, no. 4, pp. 1998-2006, Dec. 2018.

[5] Kim H D, Brown G V, Felder J L, “Distributed turboelectric propulsion for hybrid wing body aircraft”, *Proceedings of 2008 International Powered Lift Conf.*, London, United Kingdom , 2008, pp. 1-5.

[6] Felder J L, Kim H D, Brown G V, “Turboelectric distributed propulsion engine cycle analysis for hybrid-wing-body aircraft”, *47th AIAA Aerospace Sciences Meeting.* Reston, VA: AIAA, 2009, pp. 1-25.

[7] Brown G.V, “Weights and efficiencies of electric components of a turboelectric aircraft propulsion system”, *49th AIAA aerospace sciences meeting including the new horizons forum and aerospace exposition*. Reston, VA: AIAA, 2011, pp. 1-18.

[8] Nalianda.D, Singh.R, “Turbo-electric distributed propulsion opportunities, benefits and challenges”, A*ircraft Engineering and Aerospace Technology*, vol.86, no.6, pp. 543-549, Nov.2014.

[9] X. Kong, Z. Zhang, J. Lu, J. Li and L. Yu “A review of distributed electric propulsion aircraft power systems”, *Acta Aeronautica et Astronautica Sinica*, vol.35, no.x, pp. 369-391, Jan. 2017.

[10] A. Mohammadpour, A. Gandhi, and L. Parsa, “Winding factor calculation for analysis of back EMF waveform in air-core permanent magnet linear synchronous motors,” *IET Elect. Power Appl.*, vol. 6, no. 5, pp.253–259, May 2012.

[11] Weiwei Geng, Zhuoran Zhang, “Analysis and implementation of new ironless stator axial-flux permanent magnet machine with concentrated non-overlapping Windings”, *IEEE Trans. Energy. Convers.*, vol.33, no.3, pp.1274-1284, Sep. 2018.

[12] S. Javadi and M. Mirsalim, “A ironless axial-flux permanent-magnet generator for automotive applications,” *IEEE Transactions on Magnetics*, vol. 44, no. 12, pp. 4591–4598, Dec. 2008.

[13] M. Aydin and M. Gulec, “A new ironless axial flux interior permanent magnet synchronous motor with sinusoidal rotor segments,” *IEEE Trans. Magn.*, vol. 52, no. 7, pp. 1–6, Jul. 2016.

[14] Zhang, X., Bowman, C.L., O.Connell, T.C., et al, “Large electric machines for aircraft electric propulsion”, *IET Electr. Power Appl.*, vol.12, no.6, pp.767-779, Jan. 2018.

[15] R. DelRosario, "A future with hybrid electric propulsion systems: A NASA perspective," in *Proc. Turbine Eng. Technol. Symp*., Sep. 2014.

[16] Gonzalez D A, Saban D M, "Study of the copper losses in a high-speed permanent-magnet machine with form-wound windings", *IEEE Transactions on Industrial Electronics*, vol. 61, no. 6, pp. 3038-3045, Jun. 2014.

[17] Kuznetsov, S, "Machine design and configuration of a 7000 HP hybrid electric drive for naval ship propulsion", I*EEE 2011 IEEE Int. Electric Machines and Drives Conf*., Niagara Falls, 2011, pp. 1625–1628.

[18] Paulides J J H, Jewell G W, Howe D, "An evaluation of alternative stator lamination materials for a high-speed, 1.5 MW permanent-magnet generator", *IEEE Transactions on Magnetics*, vol. 40, no. 4, pp. 2041-2043, Jul. 2004.

[19] Bailey C, Saban D M, Guedes Pinto P, "Design of high-speed direct-connected permanent-magnet motors and generators for the petrochemical industry", *IEEE Transactions on Industry Applications*, vol. 45, no. 3, pp. 1159-1165, Jun. 2009.

[20] Thelen, R.F., Gattozzi, A., Wardell, D., et al, "2-MW motor and ARCP drive for high-speed flywheel", *Proc. IEEE 22nd Annual Appl. Power Electron. Conf*., Anaheim, CA, 2007, pp. 1690–1694.

[21] Pyrhonen J, Nerg J, Kurronen P, et al, "High-speed, high output, solid-rotor induction motor technology for gas compression", *IEEE Transactions on Industrial Electronics*, vol. 57, no. 1, pp. 272-280, Jan. 2010.

[22] Gieras, J.F., Saari, J, "Performance calculation for a high-speed solid-rotor induction motor", *Transactions on Industrial Electronics*, vol. 59, no. 6, pp. 2689–2700, Jun. 2012.

[23] Ahrens M, Bikle U, Gottkehaskamp. R, et al, "Electrical design of high-speed induction motors of up to 15 MW and 20000rpm", *International Conference on Power Electronics*, Bath, United Kingdom, 2002, pp. 381-386.

[24] James O, Samotyj M, Ferrier R, "Applications of high speed horsepower ASD controlled induction motors to gas pipeline" *Fifth European Conference on Power Electronics and Applications*, Brighton, 1993, pp. 430-435.

[25] Richter, E; Ferreira, C, "Performance evaluation of a 250 kW switched reluctance starter generator", *IEEE 1995 Record of the 1995, Thirtieth IAS Annual Meeting Conf., Industry Applications Conf.*, 1995, pp. 434–440.

[26] Garrigan N.R., Soong, W.L., Stephens, C.M., et al., "Radial force characteristics of a switched reluctance machine" *IEEE Thirty-Fourth IAS Annual Meeting, Conf*., 1999, pp. 2250–2258.

[27] http://www.enstroj.si/Electric-products/emrax-motorsgenerators.html

[28] Crescimbini, F., Di Napoli, A., Solero, L., et al., "Compact permanent-magnet generator for hybrid vehicle applications", *IEEE Transactions on Industry Applications*, vol. 41, no. 5, pp. 1168–1177, Jun. 2005.

[29] Caricchi, F., Maradei, F., De Donato, G., et al., "Axial-flux permanent-magnet generator for induction heating gensets", *Transactions on Industrial Electronics*, vol. 57, no. 1, pp. 128–137, Jan.2010.

[30] A. Yoon, Xuan Yi, J. Martin, Yuanshan Chen and K. Haran, "A high-speed, high-frequency, air-core PM machine for aircraft application," *2016 IEEE Power and Energy Conference at Illinois (PECI)*, Urbana, IL, 2016, pp. 1-4.

[31] N. J. Renner, J. D. Lenz, X. Yi and K. S. Haran, "Development of form-wound air-core armature windings for high-frequency electric machines," *2017 IEEE International Electric Machines and Drives Conference (IEMDC)*, Miami, FL, 2017, pp. 1-8.

[32] R. Sanchez, A. Yoon, X. Yi, Y. Chen, L. Zheng and K. Haran, "Mechanical validation of high power density external cantilevered rotor," *2017 IEEE International Electric Machines and Drives Conference (IEMDC)*, Miami, FL, 2017, pp. 1-8.

[33] D. Lee, A. Jin, B. Min, L. Zheng and K. Haran, "Optimization method to maximise torque density of high-speed slotless permanent magnet synchronous machine in aerospace applications," in *IET Electric Power Applications*, vol. 12, no. 8, pp. 1075-1081, 9 2018.

Zhuoran Zhang (M'09–SM'12) received the B.S. degree in measurement engineering and the M.S. and Ph.D. degrees in electrical engineering from Nanjing University of Aeronautics and Astronautics (NUAA), Nanjing, China, in 2000, 2003 and 2009, respectively. Since 2003, he has been a member of the faculty at Department of Electrical Engineering, NUAA, where he is currently a full professor and vice director of Jiangsu Provincial Key Laboratory of New Energy Generation and Power Conversion. From Feb. 2012 to Jun. 2013, he was a visiting professor in Wisconsin Electric Machines and Power Electronics Consortium (WEMPEC), University of Wisconsin-Madison, U.S. His research interests include design and control of permanent magnet machines, hybrid excitation electric machines, and doubly salient electric machines for aircraft power, electric vehicles and renewable energy generation. He has authored or coauthored over 130 technical papers and one book, and is the holder of 34 issued patents in these areas.

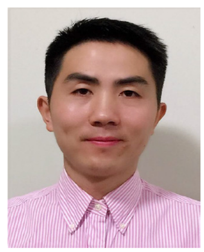

Weiwei Geng received the B.S. degree in electrical engineering from Nanjing Agricultural University (NJAU), Nanjing, China, in 2012. The M.S. and Ph.D degree in electrical engineering from Nanjing University of Aeronautics and Astronautics (NUAA), Nanjing, China, in 2014 and 2018 respectively. He has published more than 10 technical papers in journals and conference proceedings. He has eleven issued/published invention patents. His main research interests include PM machines and control, electric drive system for electric vehicles and hybrid propulsion.

Ye Liu received the B.S. degree in electrical engineering from Nanjing University of Aeronautics and Astronautics (NUAA), Nanjing, China, in 2014. He is currently working toward the Ph.D. degree in electrical engineering at NUAA, Nanjing, China. His main research interests include design and control of permanent magnet and hybrid excitation electrical machines.

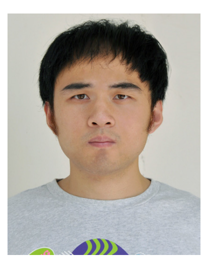

Chen Wang received the B.S. degree in electrical engineering from Xidian University, Xi'an, China, in 2010. The M.S. degree in 2013 from Jiangxi University of Science and Technology, Ganzhou, China, where he is currently working toward the Ph.D degree in electrical engineering at Nanjing University of Aeronautics and Astronautics (NUAA), Nanjing, China. His main research interests include structural design and vibration analysis of high speed machines.